Photovoltaic Power Generation with Module-Based Capacitive Energy Storage

Bowen Zheng [1], John E. Fletcher [1], Alison Lennon [2], Yu Jiang [2], Patrick A. Burr [3, *]

[1] School of Electrical Engineering and Telecommunications, UNSW Sydney, NSW 2052, Australia
[2] School of Photovoltaic and Renewable Energy Engineering, UNSW Sydney, NSW 2052, Australia
[3] School of Mechanical and Manufacturing Engineering, UNSW Sydney, NSW 2052, Australia

***Abstract* — Module-based electrochemical energy storage can be used to reduce the ramp rate of PV generation with fluctuating insolation. As the capacitance of the module-based capacitive energy storage decreases, large fluctuations on the DC link voltage are expected caused by the variation in the PV power. It is important to design and implement effective control methods to reduce this undesired effect on the DC link voltage, especially with the use of lower capacitance (1 F). A comparison of feedforward compensation, set-point weighting and anti-windup control methods based on a proportional integral (PI) controller for DC link voltage is reported. Our case studies verify the effectiveness of a PI controller combined with feedforward compensation and anti-windup scheme, and demonstrate the improvements in the DC link voltage dynamics of a single-phase grid connected system.**

***Index Terms* — Anti-windup, capacitive energy storage, DC link voltage, feedforward compensation, module-based converter, photovoltaics (PV), proportional integral (PI) controller, set-point weighting.**

I. Introduction

In recent years, photovoltaics (PV) have become an increasingly important source of electrical power generation, and the increasing penetration of PV power generation poses a set of challenges to the operation and stability of electric grids due to PV power's inherent intermittency. Electrochemical energy storage devices (ESDs) integrated in PV systems provide a possible means of meeting the grid requirements, and our recent report [1] showed that electrochemical capacitors are uncompetitive against high power batteries for centralized energy storage. However, it may be more beneficial to integrate electrochemical capacitors at the PV module-level, and a single-phase grid-connected PV system with module-based capacitive energy storage devices is introduced in [2].

Reducing the size of energy storage devices is desirable in order to decrease cost, physical size and weight of the integrated system. However, if the size of module-based energy storage devices is too small, then larger fluctuations on the DC link voltage will occur due to the unpredicted variable PV power swings. This may trigger protection devices and even shut down the operating systems when the fluctuations exceed the specified limits [3]. Therefore, in order to control the level of DC link voltage fluctuations, and at the same time, to limit the fluctuations of the intermittent PV power, it is important for the controller to ensure a quick response to sudden changes in the PV power [4]. The DC link voltage is normally kept constant, however module-based capacitors need to be charged and discharged to compensate PV power fluctuations by varying the DC link voltage in a wide range. This makes it necessary to control the transient behaviors of the variable DC link voltage [5].

Compared with complex methods, such as observer-based control [6], fuzzy logic control [7], predictive control [8], differential flatness control [9] or deadbeat control [10], proportional integral (PI) control is a straightforward approach that is typically used for most DC-link voltage control [11]–[21], including different applications varied from DC microgrid [11]–[13] to grid-connected converters [14]–[16], as well as small energy storage components [3] [17]. Among these various implementations, some executions adapt parameters in PI controllers to attenuate voltage fluctuations [15] [18]. Some PI controllers are combined with feedforward compensation [4] [11] [19], which measures and feeds the source or load power forward in the DC link voltage control scheme. This compensation greatly improves the voltage dynamic performance but at the same time increases the coupling between DC link voltage control and power control. There are also some PI controllers integrated with anti-windup schemes [20] [21], which attenuate the overshoot of DC link voltage. However, few reports focus on performance comparisons of PI-based controlled DC link voltage dynamic response, particularly between feedforward compensation, set-point weighting, anti-windup, and furthermore their respective combined control schemes, for a single-phase grid-connected PV system with small-size module-based energy storage devices.

In this paper, we compare DC link voltage dynamic response using different module-based energy storage sizes in a single-phase grid-connected PV system under power ramp rate [2] and simple PI voltage control, and demonstrate the need to improve the DC link voltage dynamic response for smaller energy storage devices, such as electrochemical capacitors. From comparisons between feedforward compensation, set-point weighting, anti-windup and their respective combinations, our case studies show that a PI controller combined with feedforward compensation plus anti-windup can greatly improve the DC link voltage dynamics. This paper is organized as follows. In Section II, a single-phase grid-connected module-based PV system and its integrated power ramp rate and DC link voltage control are introduced. In Section III, the modified

978-1-7281-0494-2/19/$31.00 ©2019 IEEE

DC link voltage control methods are discussed, and Section IV presents modelling results and compares different control schemes. Conclusions are then drawn in Section V.

II. PV System Integrated Power Ramp Rate and DC Link Voltage Control

The circuit diagram for a single-phase grid-connected PV system with module-integrated DC-DC optimizers and an inverter is shown in Fig. 1(a), and the equivalent circuit model is proposed for system-level analysis in Fig. 1(b). In order to control the ramp rate of the power injected by an array of PV modules into the AC grid, a novel control technique was proposed by utilizing the energy stored in module-based electrochemical capacitors in [2], as the control diagram illustrated in Fig. 2. To compensate for PV power excursions, the capacitor should be charged and discharged at a rate to meet the ramp rate requirements. Consequently, the inverter DC link reference voltage V^*_{INV} (equal to V^*_{ESD}, i.e., the target voltage for capacitive energy storage device) is not a constant but a controlled variable, determined from the required grid power and the energy state of the capacitor C_{ESD}, which aims to meet the PV generation ramp rate requirements by utilizing the energy stored in the capacitor. The details about the ramp rate control scheme are discussed in [2], where a proportional (P) controller was used. Since the reference voltage is calculated based on the following equation,

$$V^*_{\mathrm{INV}}(t)=\sqrt{{V^*_{\mathrm{INV}}}^2(t-\Delta t)+\frac{2\left[E_{\mathrm{ESD}}(t)-E_{\mathrm{ESD}}(t-\Delta t)\right]}{C_{\mathrm{ESD}}}} \tag{1}$$

for the same amount of energy compensation, a larger change of the reference voltage is required when the capacitance is decreased, i.e., the change of V^*_{INV} is more frequent for the small capacitance (e.g., 1 F) when it is compared with the large capacitance (e.g., 100 F). To further reduce steady-state errors for small capacitance, with the use of a typical PI controller, the

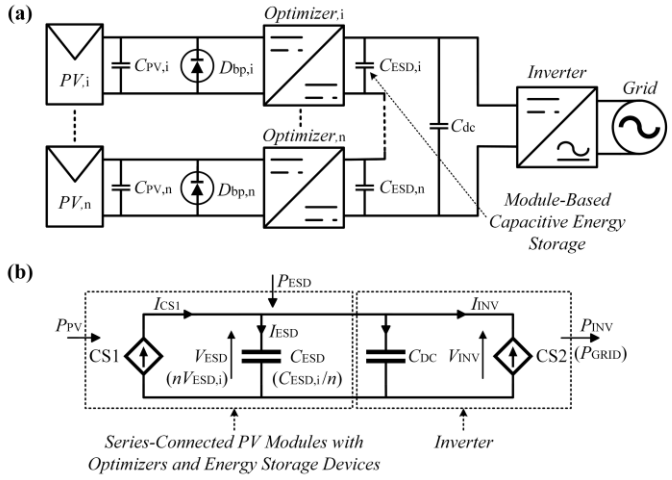

Fig. 1. (a) Single-phase grid-connected PV system with module-integrated DC-DC optimizer, inverter and module-based capacitive energy storage $C_{\mathrm{ESD,i}}$. (b) Proposed equivalent circuit model for a single-phase grid-connected PV system.

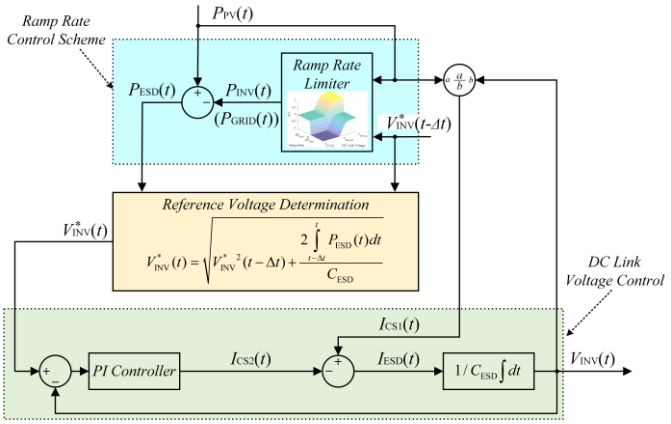

Fig. 2. Integration of power ramp rate control and inverter DC link voltage control for PV system with module-based capacitive energy storage devices.

transfer function of the inverter DC link voltage can be described as

$$\frac{V_{\mathrm{INV}}}{V^*_{\mathrm{INV}}}=\frac{K_{\mathrm{P}}s+K_{\mathrm{I}}}{C_{\mathrm{ESD}}s^2+K_{\mathrm{P}}s+K_{\mathrm{I}}} \tag{2}$$

where the zero is always held as $z = -K_{\mathrm{I}}/K_{\mathrm{P}}$. Compared with the standard second order transfer function, the relations are derived as follows,

$$K_{\mathrm{P}}=2\zeta\omega_{\mathrm{n}}C_{\mathrm{ESD}} \tag{3}$$

$$K_{\mathrm{I}}=\omega_{\mathrm{n}}^2C_{\mathrm{ESD}} \tag{4}$$

where ζ is damping ratio, and ω_{n} is natural frequency. In addition, the relation between current change ΔI_{CS1} and voltage change ΔV_{INV} can be derived as

$$\Delta V_{\mathrm{INV}}=\frac{s}{C_{\mathrm{ESD}}s^2+K_{\mathrm{P}}s+K_{\mathrm{I}}}\Delta I_{\mathrm{CS1}} \tag{5}$$

which indicates that with the decrease of capacitance, the voltage deviation caused by the sudden change of current (PV power) is increased. Therefore, it is important to use more effective control techniques to regulate the DC link voltage for small-size capacitors, and three different control methods are introduced in the next section.

III. Modified DC Link Voltage Control

Based on the PI control for DC link voltage, three additional methods are proposed to improve the voltage dynamic response. These include: (i) feedforward compensation; (ii) set-point weighting; and (iii) anti-windup. The modified control scheme is shown in Fig. 3. The performance of these control methods is considered alone and in combination with other of voltage control methods.

A. Feedforward Compensation

In order to improve the control system dynamic response and reduce the energy storage capacitance at the same time, one way is to have a faster control system. Feedforward control has an open-loop nature, and its dynamic response is faster than the

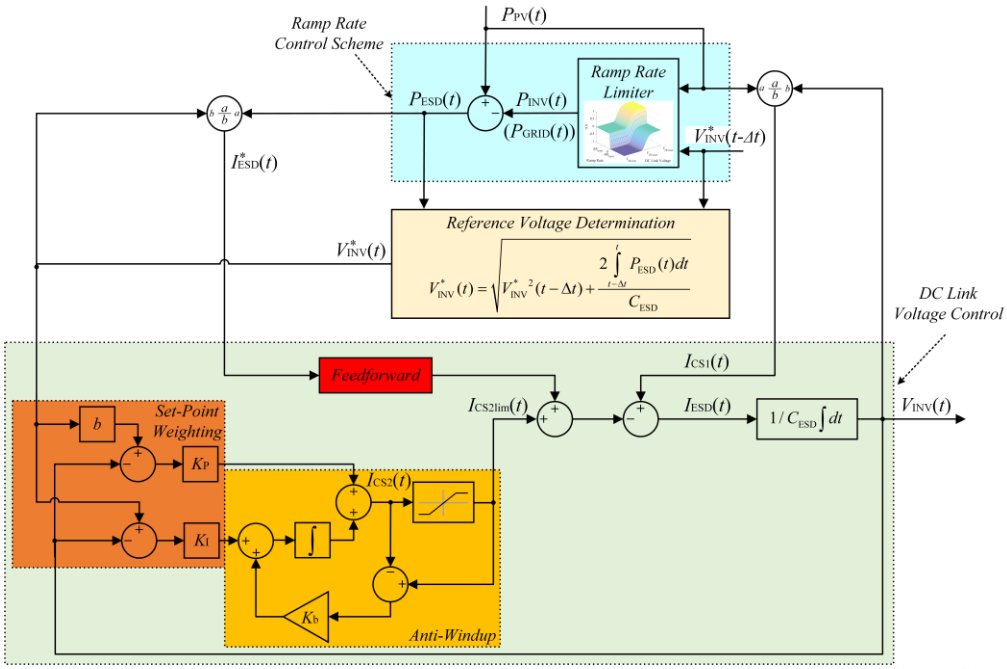

Fig. 3. Integration of power ramp rate control and modified inverter DC link voltage control for PV system with module-based capacitive energy storage devices, including feedforward compensation, set-point weighting and anti-windup.

feedback loop control [6]. Here, the current I^*_{ESD} is used for feedforward compensation, where

$$I^*_{ESD} = \frac{P^*_{ESD}}{V^*_{INV}} \tag{6}$$

and P^*_{ESD} and V^*_{INV} are target power and voltage for capacitor, which are calculated and obtained based on the ramp rate control, i.e., the target current I^*_{ESD} is determined and fed forward to the capacitor. With the feedforward compensation, the transfer function of DC link voltage can be represented as

$$V_{INV} = \frac{K_P s + K_I}{C_{ESD} s^2 + K_P s + K_I} V^*_{INV} + D \tag{7}$$

where D represents the disturbance component. Assuming that under the steady state, the measured voltage V_{INV} is equal to the reference voltage V^*_{INV}, and the disturbance can be approximated as

$$D = \frac{s}{C_{ESD} s^2 + K_P s + K_I}\left(\frac{P_{INV}}{V^*_{INV}}\right) \tag{8}$$

Compared with the disturbance without compensation in (9),

$$D = \frac{s}{C_{ESD} s^2 + K_P s + K_I}\left(\frac{P_{PV}}{V_{INV}}\right) \tag{9}$$

the disturbance with feedforward compensation in (8) helps to make the disturbance small, since the fluctuations of the power fed to inverter P_{INV} are much attenuated compared with PV power P_{PV} with the implementation of ramp rate control scheme [2].

B. Set-Point Weighting

Another common technique to improve dynamic response based on a PI controller is set-point weighting. With the set point and the process output separate, the errors in the proportional part e^P_{INV} and integral part e^I_{INV} are calculated respectively as

$$e^P_{INV} = bV^*_{INV} - V_{INV} \tag{10}$$

$$e^I_{INV} = V^*_{INV} - V_{INV} \tag{11}$$

where the parameter b ($0 \le b \le 1$) is the set-point weight. The desired set-point response could be simply maintained by adjusting the set-point weight [22], which could be chosen so that the largest gain of the transfer function is one or close to one, helping to avoid overshoot for system. Therefore, the output of the PI controller can be described as

$$u = K_P\left(bV^*_{INV} - V_{INV}\right) + \frac{K_I}{s}\left(V^*_{INV} - V_{INV}\right) \tag{12}$$

and the weighted set-point PI controller can be represented as

$$\frac{V_{INV}}{V^*_{INV}} = \frac{bK_P s + K_I}{C_{ESD} s^2 + K_P s + K_I} \tag{13}$$

The parameter b influences the position of zero, i.e., $z = -K_I/bK_P$, and the suitable choice of b reduces the overshoot (i.e., the zero is moved away from the imaginary axis to reduce the overshoot and settling time). Since only the zero of the transfer function is changed but not the pole, the closed-loop stability is not affected by set point weighting [23]. However, the too small value of b decreases the rise time and slows down the response [24]. Consequently, the main disadvantage of this method is that the reduction of the overshoot is paid by a slower set-point response, and the effectiveness of the proportional action is somewhat reduced.

C. Anti-Windup

Since the DC link voltage is required to vary within a range [V_{INVmin}, V_{INVmax}] for charging and discharging the capacitors, the control variable I_{CS2} could reach the limits, which leads the feedback loop broken and the system running as an open loop. Due to the use of integral action of the PI controller, the error may continue to be integrated caused by large set-point changes or significant disturbances. If the control algorithm is not designed properly, the integral term may become very large, which is called integral windup, also known as integrator windup or reset windup, and the integral term accumulates a significant error, with the overshoot continuing increased as the accumulated error is unwound. In another way, any controller with integral action may give large transients when the actuator saturates [22]. To avoid this, an anti-windup scheme based on back-calculation is implemented in Fig. 3. As the output saturates, the integral term in the controller is recomputed so that its new value gives an output at the saturation limit, which dynamically resets the integrator with the anti-windup gain K_{b}. Specifically, an extra feedback path is generated by measuring the output of the controller I_{CS2} and the actuator output I_{CS2lim}, which forms an error signal fed to the input of the integrator through K_{b}. The integrator input is

$$K_{\mathrm{I}}\left(V_{\mathrm{INV}}^{*}-V_{\mathrm{INV}}\right)+K_{\mathrm{b}}\left(I_{\mathrm{CS2lim}}-I_{\mathrm{CS2}}\right) \tag{14}$$

Hence,

$$I_{\mathrm{CS2lim}}-I_{\mathrm{CS2}}=-\frac{K_{\mathrm{I}}}{K_{\mathrm{b}}}\left(V_{\mathrm{INV}}^{*}-V_{\mathrm{INV}}\right) \tag{15}$$

Therefore, it follows that

$$I_{\mathrm{CS2}}=I_{\mathrm{CS2lim}}+\frac{K_{\mathrm{I}}}{K_{\mathrm{b}}}\left(V_{\mathrm{INV}}^{*}-V_{\mathrm{INV}}\right) \tag{16}$$

where the signals I_{CS2lim} and $(V_{\mathrm{INV}}^{*}-V_{\mathrm{INV}})$ always have the same sign, and I_{CS2} is always larger than I_{CS2lim} in magnitude. This prevents the integrator from winding up, and the rate at which the controller output is reset is governed by the anti-windup gain K_{b}, and $1/K_{\mathrm{b}}$ can be interpreted as the time constant of anti-windup loop, which determines how quickly the integral is reset. As (16) indicates, to reach steady state quickly under saturation conditions, K_{b} must be very high [25].

IV. Modelling Results

A. Capacitance Size Comparison

For our case studies, irradiance data with one-second resolution for 1000 s during one of the most fluctuating day (Day A in [2]) is chosen for analysis, and the PV power is depicted in Fig. 4. In order to compare the effects of capacitance size on voltage dynamic response under the integrated PV power ramp rate and DC link voltage control, which are illustrated in Fig. 2, two different capacitances, i.e., $C_{\mathrm{ESD,i}}=100$ F and 1 F, are chosen for testing. The modelling and control parameters for the PV system are listed in Table I.

TABLE I
Parameters for PV System Modelling and Control

Symbol	Parameter	Value
V_{INVnom}	DC Link Nominal Voltage	31.4 V
P_{PVrated}	PV Rated Power	280 W
ζ	Damping Ratio	0.707
ω_{n}	Natural Frequency	0.628 rad/s
b	Set-Point Weight	0.8
K_{b}	Anti-Windup Gain	100

Fig. 5 shows the DC link voltage dynamic response for two module-based capacitors, and the red and black lines represent the reference voltage V_{INV}^{*} and the measured voltage V_{INV} respectively. With 100 F module-based capacitors (Fig. 5(a)), the change of V_{INV}^{*} is much slower than that of 1 F capacitors (Fig. 5(b)), and the DC link voltage V_{INV} can be accurately tracked with the reference V_{INV}^{*} only using a PI controller. As the capacitance is decreased to 1 F, the reference voltage V_{INV}^{*} is changed much faster and bounded within the limits, which causes notable overshoots and oscillations of the DC link voltage. In addition, compared with 100 F capacitors, the DC link voltage is more vulnerable to the disturbances (sudden change of PV power) when the capacitance is 1 F, which indicates that more effective control methods should be designed and implemented for reducing the undesired effects on the DC link voltage caused by the use of small-size capacitors.

B. DC Link Voltage Control Comparison

To improve the dynamics of DC link voltage, especially for small-size module-based capacitors, based on the implementation of DC link voltage only using a PI controller, additional three control techniques (feedforward compensation, set-point weighting and anti-windup) are tested separately for 1 F capacitors, and the improvements of the DC link voltage are compared in Fig. 6, where the first 100 s are chosen for closer observations. Fig. 6(a) shows that as a change of the DC link reference voltage is forced from its nominal voltage (31.4 V) to its maximum (38.4 V), the overshoot of the dynamic response could reach around 47.4 V with the use of a single PI controller. Then, as the PV power suddenly changes at around 65 s, the DC link voltage starts to fluctuate, indicating the influences of disturbances as well as the limitations of a single PI controller on DC link voltage. Therefore, with the addition of feedforward compensation, Fig. 6(b) shows the improvement of the DC link voltage dynamic response, especially on attenuating the

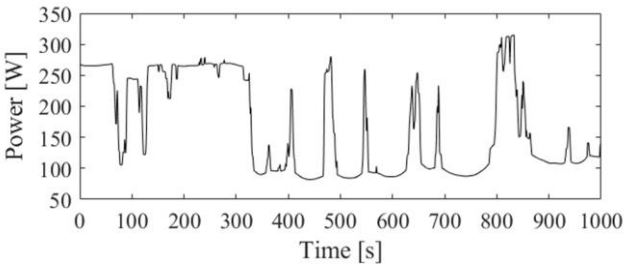

Fig. 4. PV power for 1000 s during one fluctuating day (Day A in [2]), which are based on solar irradiance data with one-second resolution.

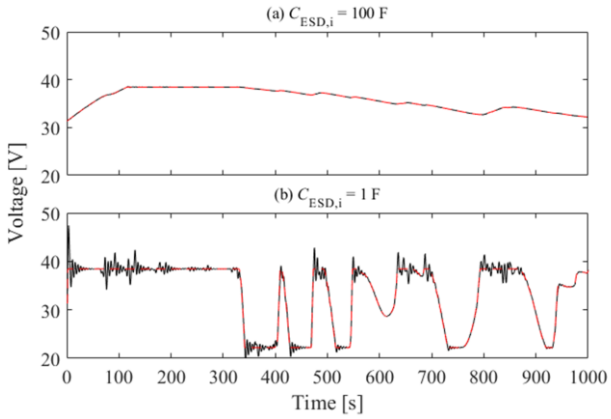

Fig. 5. Comparison of DC link voltage between different module-based capacitance (a) $C_{ESD,i}$ = 100 F and (b) $C_{ESD,i}$ = 1 F under the simple PI DC link voltage control, where the red and black lines represent the reference voltage V_{INV}^{*} and the measured voltage V_{INV} respectively.

influences of current disturbances, which evinces the effectiveness of feedforward compensation. In addition, Fig. 6(c) evaluates the effect of set-point weighting, and it shows that the overshoot is reduced to about 42.6 V. However, as discussed in Section III, compared with Fig. 6(a), the set-point weighting in Fig. 6(c) delays the response. With regard to the benefits of anti-windup, even though the overshoot peak of the voltage response in Fig. 6(d) is nearly the same as that with only using a PI controller, the subsequent oscillations are reduced at a faster rate, which therefore takes a shorter time for the DC link voltage to be tracked to its reference.

There are still some limitations with the implementation of single compensation schemes. Instead of applying the methods individually, different combinations of these three methods are investigated, and the corresponding comparisons are shown in Fig. 7. Compared with other three combinations in Fig. 7 (b) – (d), Fig. 7(a) indicates that without feedforward compensation, the DC link voltage is more vulnerable to PV power fluctuations, and this emphasizes the importance of

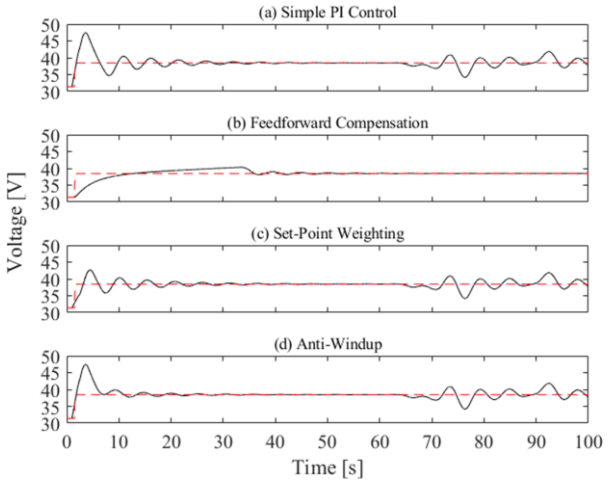

Fig. 6. Comparison of DC link voltage between different control methods, including (a) simple PI control, with (b) feedforward compensation, (c) set-point weighting and (d) anti-windup.

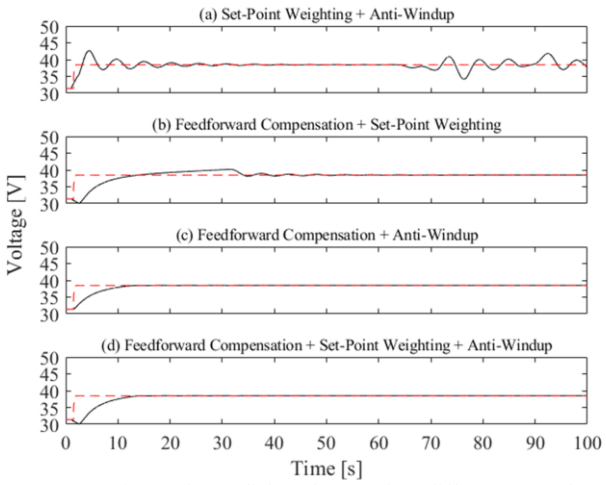

Fig. 7. Comparison of DC link voltage using different control method combinations, including (a) set-point weighting and anti-windup, (b) feedforward compensation and set-point weighting, (c) feedforward compensation and anti-windup and (d) integrated three control methods.

feedforward compensation for power smoothing. Fig. 7(b) shows that the voltage dynamic response is nearly the same as that in Fig. 6(b), demonstrating that the feedforward compensation dominates the control, and the response delay is caused by using set-point weighting. Comparisons between Fig. 7(c) and (d) indicate that combination of feedforward compensation and anti-windup has better performance of the DC link voltage dynamics, where set-point weighting still delays the response in Fig. 7(d). Therefore, a PI controller with feedforward compensation plus anti-windup is suggested to be implemented to improve the DC link dynamics for a single-phase grid-connected PV system with small-size module-based energy storage devices.

V. Conclusions

In a single-phase grid-connected PV system, module-based electrochemical capacitors can be used to reduce the ramp rate of PV generation in the presence of fluctuating insolation. With simple PI voltage control, it is necessary to design and implement more effective control methods to improve the DC link voltage dynamic response for systems with smaller energy capacitances. Based on the comparisons of a PI controller combined with feedforward compensation, set-point weighting, anti-windup and their respective combinations, our simulation results show that the PI-based control with feedforward compensation plus anti-windup can greatly improve the DC link voltage dynamics for a single-phase grid-connected PV system, especially with small-capacitance systems.

References

[1] Y. Jiang et al., "Suitability of representative electrochemical energy storage technologies for ramp-rate control of photovoltaic power," *J. Power Sources*, vol. 384, pp. 396–407, 2018.

[2] B. Zheng, J. E. Fletcher, A. Lennon, Y. Jiang, and P. A. Burr, "Improving generation ramp rates of photovoltaic systems using module-based capacitive energy storage," *J. Power Sources*, vol. 423, pp. 227–235, 2019.
[3] S. A. Khajehoddin, M. Karimi-Ghartemani, P. K. Jain, and A. Bakhshai, "DC-bus design and control for a single-phase grid-connected renewable converter with a small energy storage component," *IEEE Trans. Power Electron*., vol. 28, no. 7, pp. 3245–3254, 2013.
[4] M. Ciobotaru, R. Teodorescu, and F. Blaabjerg, "Control of single-stage single-phase PV inverter," *EPE J. (European Power Electron. Drives Journal)*, vol. 16, no. 3, pp. 20–26, 2006.
[5] C. Y. Yu, J. Tamura, and R. D. Lorenz, "Optimum dc bus voltage analysis and calculation method for inverters/motors with variable dc bus voltage," *IEEE Trans. Ind. Appl*., vol. 49, no. 6, pp. 2619–2627, 2013.
[6] C. Wang, X. Li, L. Guo, and Y. W. Li, "A nonlinear-disturbance-observer-based DC-bus voltage control for a hybrid AC/DC microgrid," *IEEE Trans. Power Electron*., vol. 29, no. 11, pp. 6162–6177, 2014.
[7] H. Kakigano, Y. Miura, and T. Ise, "Distribution voltage control for DC microgrids using fuzzy control and gain-scheduling technique," *IEEE Trans. Power Electron*., vol. 28, no. 5, pp. 2246-2258, 2013.
[8] A. Kotsopoulos, J. L. Duarte and M. A. M. Hendrix, "Predictive DC voltage control of single-phase PV inverters with small DC link capacitance," *2003 IEEE International Symposium on Industrial Electronics (Cat. No.03TH8692)*, Rio de Janeiro, Brazil, 2003, pp. 793-797 vol. 2.
[9] P. Thounthong, "Model based-energy control of a solar power plant with a supercapacitor for grid-independent applications," *IEEE Trans. Energy Convers*., vol. 26, no. 4, pp. 1210–1218, 2011.
[10] B. Wang, U. Manandhar, X. Zhang, H. B. Gooi, and A. Ukil, "Deadbeat control for hybrid energy storage systems in DC microgrids," *IEEE Trans. Sustain. Energy*, 2018.
[11] P. Karlsson and J. Svensson, "DC bus voltage control for a distributed power system," *IEEE Trans. Power Electron*., vol. 18, no. 6, pp. 1405–1412, 2003.
[12] D. Chen and L. Xu, "Autonomous DC voltage control of a DC microgrid with multiple slack terminals," *IEEE Trans. Power Syst*., vol. 27, no. 4, pp. 1897–1905, 2012.
[13] S. K. Kollimalla et al., "DC grid voltage regulation using new HESS control strategy," *IEEE Trans. Sustain. Energy*, vol. 8, no. 2, pp. 772–781, 2017.
[14] S. Taghizadeh, J. Hossain, J. Lu, and M. Karimi Ghartemani, "An enhanced DC-bus voltage control loop for single-phase grid-connected DC/AC converters," *IEEE Trans. Power Electron*., vol. 34, no. 6, pp. 5819-5829, 2019.
[15] M. Merai, M. W. Naouar, and I. Slama-Belkhodja, "An improved DC-link voltage control strategy for grid connected converters," *IEEE Trans. Power Electron*., vol. 33, no. 4, pp. 3575–3582, 2018.
[16] L. Zhang, K. Sun, Y. Xing, L. Feng, and H. Ge, "A modular grid-connected photovoltaic generation system based on DC bus," *IEEE Trans. Power Electron*., vol. 26, no. 2, pp. 523–531, 2011.
[17] M. Karimi-Ghartemani, S. A. Khajehoddin, P. Jain, and A. Bakhshai, "A systematic approach to DC-bus control design in single-phase grid-connected renewable converters," *IEEE Trans. Power Electron*., vol. 28, no. 7, pp. 3158–3166, 2013.
[18] M. Merai, M. W. Naouar, I. Slama-Belkhodja, and E. Monmasson, "An adaptive PI controller design for DC-link voltage control of single-phase grid-connected converters," *IEEE Trans. Ind. Electron*., vol. 66, no. 8, pp. 6241–6249, 2019.
[19] B. G. Gu and K. Nam, "A DC-link capacitor minimization method through direct capacitor current control," *IEEE Trans. Ind. Appl*., vol. 42, no. 2, pp. 573–581, 2006.
[20] J. Rocabert, R. Capo-Misut, R. S. Munoz-Aguilar, J. I. Candela, and P. Rodriguez, "Control of energy storage system integrating electrochemical batteries and supercapacitors for grid-connected applications," *IEEE Trans. Ind. Appl*., vol. 55, no. 2, pp. 1853–1862, 2019.
[21] M. B. Camara, B. Dakyo, and H. Gualous, "Polynomial control method of DC/DC converters for DC-bus voltage and currents management-battery and supercapacitors," *IEEE Trans. Power Electron*., vol. 27, no. 3, pp. 1455–1467, 2012.
[22] K. J. (Karl J. Åström and T. Hägglund, *Advanced PID control*. ISA-The Instrumentation, Systems, and Automation Society, 2006.
[23] Chang-Chieh Hang and Lisheng Cao, "Improvement of transient response by means of variable set point weighting," *IEEE Trans. Ind. Electron*., vol. 43, no. 4, pp. 477–484, 1996.
[24] G. Prashanti and M. Chidambaram, "Set-point weighted PID controllers for unstable systems," *J. Franklin Inst*., vol. 337, no. 2–3, pp. 201–215, 2000.
[25] A. Ghoshal and V. John, "Anti-windup schemes for proportional integral and proportional resonant controller," *Natl. Power Electron. Conf. 2010*, no. 2, pp. 1–6, 2010.